Available online at www.sciencedirect.com
SCIENCE DIRECT®
Journal of Power Sources 133 (2004) 126–134
JOURNAL OF POWER SOURCES
www.elsevier.com/locate/jpowsour

Failure mode of valve-regulated lead-acid batteries under high-rate partial-state-of-charge operation

L.T. Lam*, N.P. Haigh, C.G. Phyland, A.J. Urban

CSIRO Energy Technology, Bayview Avenue, Clayton South, Vic. 3169, Australia

Received 8 August 2003; accepted 19 November 2003

Abstract

Within the next decade, there will be major changes in automotive technology with the introduction of several new features which will increase significantly the on-board power requirements. This high power demand is beyond the capability of present 14 V alternators and thus a 42 V power network is to be adopted. The new 'PowerNet' requires the lead-acid battery to be capable of providing a large number of shallow discharge–charge cycles at a high rate. High-rate discharge is necessary for engine cranking and power assist, while high-rate charge is associated with regenerative braking. The battery will operate at these high rates in a partial-state-of-charge condition, so-called HRPSoC duty.

Under simulated HRPSoC duty, it is found that the valve-regulated lead-acid (VRLA) battery fails prematurely due to the progressive accumulation of lead sulfate mainly on the surfaces of the negative plates. This is because the lead sulfate cannot be converted efficiently back to sponge lead during charging either from the engine or from regenerative braking. Eventually, the layer of lead sulfate develops to such extent that the effective surface area of the plate is reduced markedly and the plate can no longer deliver the high cranking-current demanded by the automobile.

A mechanistic analysis of battery operation during HRPSoC duty shows that high-rate discharge is the key factor responsible for the build-up of the lead sulfate layer. Such discharge causes a compact layer of tiny lead sulfate crystals to form on the surface of the negative plate and subsequent charging gives rise to an early evolution of hydrogen. Hydrogen evolution is further exacerbated when a high charging current is used.

Keywords: The 42 V PowerNet; Failure mode; High-rate partial-state-of-charge duty; Hydrogen evolution; Lead-acid battery; Sulfation

1. Background

1.1. Automotive electrical systems—the need for change

Around 1960, the voltage of automotive batteries was increased from 6 to 12 V (Fig. 1). This change was necessary because the battery was required to provide basic power and energy not only for starting, lighting and ignition of the vehicle ('SLI duty'), but also for numerous, add-on, electronic devices (e.g., radio/cassette recorder, air-conditioning, power steering, power windows). Since then, 12 V lead-acid batteries have been used widely in passenger cars, vans and trucks. Consequently, batteries have become more reliable and more durable with the result that routine/regular maintenance has been largely eliminated. Furthermore, specific energy and specific power have both been increased to allow some reduction in battery weight and to accommodate more comfort and safety features in vehicles, particularly in luxury cars (e.g., electrically operated/heated seats, navigation aids, television/sound systems, zone comfort control, traction control, electronically controlled suspension, anti-lock braking). Today, standard automotive batteries have capacities of between 40 and 60 Ah, weigh about 13 kg, and deliver 400–500 A necessary to start engines. The batteries are supported and maintained by a system voltage of between 14 and 15 V, with a generator capacity of maximum output ~2 kW.

Within the next decade, there will be major changes in automotive technology with the introduction of several new features that will increase significantly the on-board power requirements and introduce other advantages such as [1]:

- *Simplified electrical architecture*
  - wiring and wiring-loom variants will be decreased considerably by the introduction of a bus system;

* Corresponding author. Tel.: +61-3-9545-8401; fax: +61-3-9545-8403.
E-mail address: lan.lam@csiro.au (L.T. Lam).

0378-7753/$ – see front matter © 2003 Published by Elsevier B.V.
doi:10.1016/j.jpowsour.2003.11.048

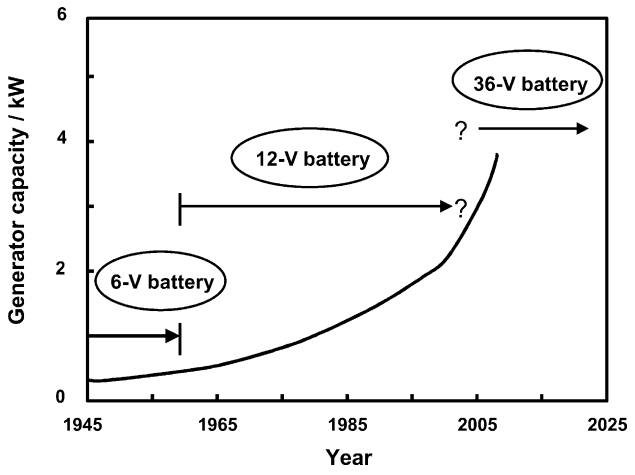

Fig. 1. Evolution of battery voltage in automobiles.

- repair and maintenance will be made easy with a universal diagnostic tool.

- *Enhanced vehicle services*
  - network capability with outside world (e.g., send/receive e-mail, internet connection via voice activation);
  - further increases in driver comfort (e.g., electrochromic windows) and vehicle safety (e.g., collision-avoidance devices, blind-spot sensors).
- *Lower fuel consumption and emissions*
  - de-coupling of many of the existing components of the vehicle system (e.g., water and oil pumps, power-assisted steering and braking) from the internal-combustion engine and conversion to electric drive (x-by-wire);
  - introduction of an integrated starter and generator (ISG) to optimize engine management and provide the ability to stop and start the engine during short stationary (idle) periods;
  - electromagnetic control of engine valves to dispense with camshafts and the large-toothed timing belts which drive the camshafts;
  - improvement of electrically heated catalytic converters with pre-heaters.

Forecasts of the electrical demand in cars fitted with these advanced features indicate a three-fold increase in the average power and a five-fold increase in the peak power. The higher power demand is beyond the capability of present 14 V alternators and thus it is proposed to adopt a 42 V power network ('PowerNet'). The voltage of the new network is a compromise between the need for higher efficiency from the electrical and electronic components, and the need for compliance with safety requirements. Clearly, the higher voltage enables power to be obtained at lower currents. This will reduce losses in electricity transmission and allow the use of components (cabling, semiconductors, etc.) of much lower cost.

The 42 V PowerNet is particularly attractive for luxury cars because these models have already been equipped with extensive electronic components which have a combined power demand that is close to the limit of the present 14 V alternator. It is clear that the need for higher power will grow for mid-size to luxury cars, as has been experienced in the past. Recently, several thousand Toyota *Crown* cars have been fitted with 42 V PowerNets. It is claimed that this 'mild' hybrid vehicle gives an overall 15% reduction in fuel consumption compared with the conventional version. In fact, fuel savings of about 25% have been achieved when driving in the heavy traffic of urban areas.

1.2. Performance criteria for battery system

To meet the growing demands on automotive electrical supplies, the new 42 V systems will require 36 V batteries with the following enhanced characteristics.

- Higher power to allow the introduction of new cranking techniques, ISGs, and pre-heatable catalyst converters; this power must be achieved without appreciable increases in battery size and weight. (Note, pulse power levels of up to 10 kW are expected.)
- Greater specific energy to support the increased number of services and controls during engine-off periods.
- Guaranteed long service-life under high-rate partial-state-of-charge (HRPSoC). Note, the increased number of service and control features is likely to result in more extensive cycling of the battery.

The introduction of an ISG is likely to provide the capability of frequent stop–start operation during journeys (i.e., during idling periods) and will, therefore, improve fuel economy. Under such conditions. The battery must accept charge efficiently via the regenerative-braking system, and must be capable of providing a large number of shallow discharge cycles. Because of its low cost and high recycling capability, lead-acid appears to be the obvious choice for the standard 42 V PowerNet, but there are shortcomings in battery reliability and cycle-life.

The objective of this study is to determine the failure mode and to understand the failure mechanism of valve-regulated lead-acid (VRLA) batteries operated under the simulated HRPSoC duty. This information is essential for future improvement of battery reliability.

2. Experimental

2.1. The 42 V profile (HRPSoC cycling)

Studies were conducted on 12 V, commercial VRLA batteries (C_{20} = 33 Ah). One cell of each battery was fitted with a $Hg|Hg_2SO_4$ reference electrode. The batteries were then subjected to the 42 V profile shown in Fig. 2 [2–5]. The duration of the profile is short, namely, 2.35 min. The profile is composed of several current steps that simulate the power required from the battery during vehicle operation,

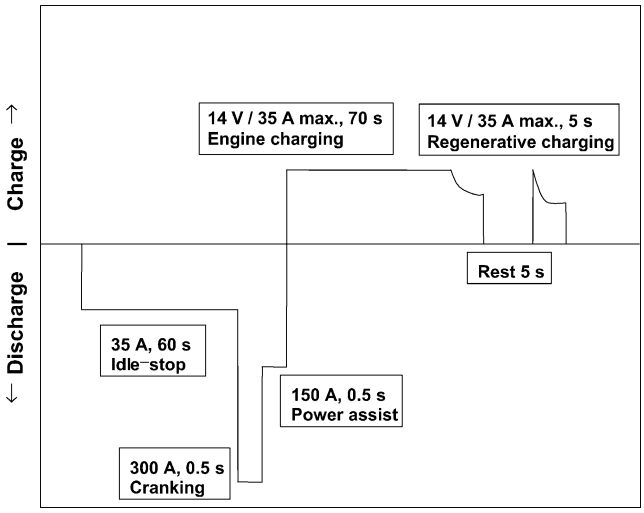

Fig. 2. The 42 V profile used for testing batteries under simulated HRP-SoC.

i.e., idle-stop, cranking, power assist, engine charging, and regenerative charging. The critical steps are the cranking and regenerative charging periods. During cranking, the battery must deliver a current of 300 A for 0.5 s, i.e., a current equal to $\sim 18C_1$.

The batteries were placed in a water bath which was maintained at 40 °C. Prior to the test, the batteries were brought to a fully charged state by applying a maximum current of 2.5 A and a constant voltage of 14.7 V for a total of 24 h. The batteries were then subjected to repetitive applications of the 42 V profile. Each application was considered to be 'one cycle' and a maximum of 1200 cycles was applied. The test was terminated when the batteries could not sustain at least 960 cycles (i.e., 80% of 1200 cycles) due to decrease in the end-of-discharge voltage to the cut-off value of 9.6 V during cycling. Otherwise, the batteries were charged fully and then subjected to a further set of 1200 cycles.

2.2. Teardown analysis

After battery failure under the 42 V profile, a detailed examination was conducted to determine the distribution of lead sulfate across cross-sections of negative and positive plates in both discharged and charged states. The samples, which were taken from plates in the outermost cell below the negative terminal, were mounted in epoxy resin to allow preparation of polished cross-sections for electron probe micro-analysis (EPMA). The five remaining cells in the battery were then subjected to a full charge. After charging, samples were taken from the cell adjacent to the outermost cell and then prepared for EPMA by means of the same procedure as that used for discharged samples. Thus, obviously, samples in discharged and charged states were obtained from different plates in different cells. Data on elemental abundance were acquired with a Joel Model JXA-8900R Superprobe which was operated at an accelerating voltage of 15 kV and a nominal beam current of 50 nA. Analyses were conducted for lead, sulfur, and oxygen.

3. Results and discussion

3.1. Performance of VRLA batteries under 42 V profile

Battery VR1 was prepared and subjected to the 42 V profile. After completing eight sets of the profile, the batteries could withstand only about 700 cycles on the ninth set (Fig. 3). Within each set, the charge-to-discharge ratio (c:d ratio) of the battery is always low initially (~0.7), but increases rapidly to a value of ~1.03. For a given set, the internal resistance of the battery increases with cycling. Furthermore, this change in internal resistance increases with the application of successive sets. For example, the internal resistance reaches 9.4 mΩ in the ninth set as opposed to 7.5 mΩ in the first set. The increase in internal resistance with cycling suggests a build-up of lead sulfate in the

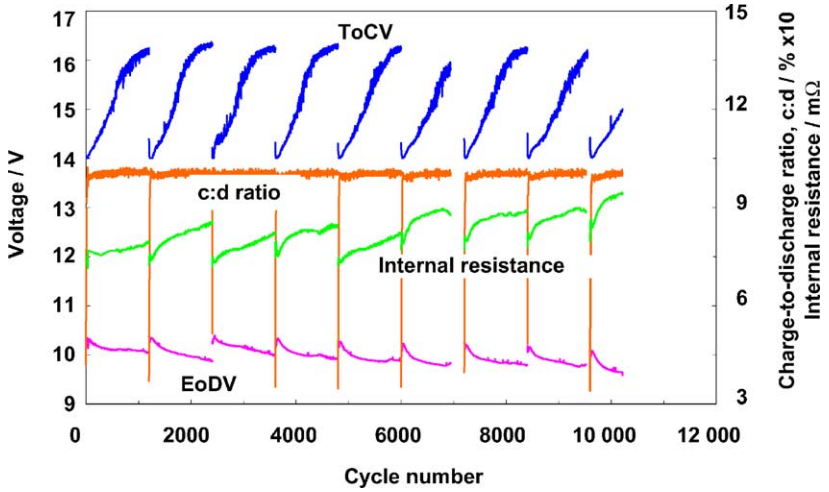

Fig. 3. Performance of VRLA battery VR1 under repetitive 42 V duty: ToCV, top-of-charge voltage; EoDV, end-of-discharge voltage.

negative/positive plates which cannot be reduced/oxidized completely even during full charging.

The end-of-discharge voltage (EoDV) of the battery decreases slowly during individual sets of cycling and reaches the cut-off value of 9.6 V during the ninth set. On the other hand, the top-of-charge voltage (ToCV) of the battery during each set is about 14.2 V initially, but starts to increase after 30 cycles and reaches a value as high as 16.5 V. This is due to overshoot of the voltage during the early stages of the regenerative-charging period.

The 42 V profile includes two periods of charging: one from the engine and the other from regenerative braking (Fig. 2). Both charging procedures are regulated at a voltage of 14 V. During engine charging, the battery voltage increases and stays at 14 V. During regenerative charging, however, the battery voltage shoots rapidly above the regulated value in the early stages (i.e., within <200 ms), and then decreases and remains at 14 V. Within a given set, the degree of voltage overshoot increases with cycling (Fig. 3). This phenomenon is similar to that observed for VRLA batteries under hybrid electric vehicle duty [6]. Battery VR1 completed 10 300 cycles before failure.

In order to confirm the consistency of the results, a second battery, VR2, was prepared and subjected to the same test. The performance of battery VR2 is very close to that of battery VR1, namely, 10 441 versus 10 300 cycles (Fig. 4). There is a difference, however, in the ToCV values. Compared with battery VR1, the rate of increase in the ToCV of battery VR2 is slower and the maximum value is lower during each set of cycling (i.e., 15.7 V for battery VR2 versus 16.3 V for battery VR1).

As mentioned above, the critical steps in the 42 V profile are the cranking and the regenerative-charging periods. Therefore, it is important to determine which plate polarity is responsible for the decrease (cranking) and overshoot (regenerative charging) of the cell voltage during cycling. Changes in the negative- and positive-plate potentials during each step of the 42 V profile are shown in Fig. 5 for the 6000th cycle of battery VR2. Clearly, during engine cranking, the negative plate experiences a much greater decrease in potential than its positive counterpart. The negative-plate potential rises rapidly during the early stages of regenerative charging (i.e., <200 ms), but then decreases. This indicates that both the charge and discharge of the battery under 42 V duty is 'negative-potential limited'.

3.2. Teardown analysis

The distribution of lead sulfate across the cross-section at the central top of a negative plate from battery VR2 is shown in Fig. 6. In the discharged state (Fig. 6(a)), lead sulfate concentrates on the surface of the plate, little is present in the interior. (Note, in this particular sample, the lead sulfate has developed predominantly on one side of the plate.) After charging, lead sulfate still remains on the surface of the plate and on the walls of the pores. Similar features were observed for samples taken from the central bottom of the negative plate (Fig. 7). Clearly, charging is unable to convert all of the lead sulfate back to sponge lead.

The distribution of lead sulfate at the central bottom of a positive plate removed from battery VR2 is shown in Fig. 8. Lead sulfate also develops mainly on the surfaces of positive plates in the discharged state, but is almost completely converted to lead dioxide after charging.

From the above observations, it can be concluded that failure of the VRLA batteries under the 42 V profile is due to the accumulation of lead sulfate on the surfaces of the negative plates. The sulfate builds up to such extent that the plates can no longer deliver the high cranking-current required by the 42 V duty.

3.3. Mechanism of lead sulfate accumulation in negative plates under HRPSoC duty

The discharge and charge processes of the negative plate can be expressed by the reactions (1)–(4) shown in Fig. 9.

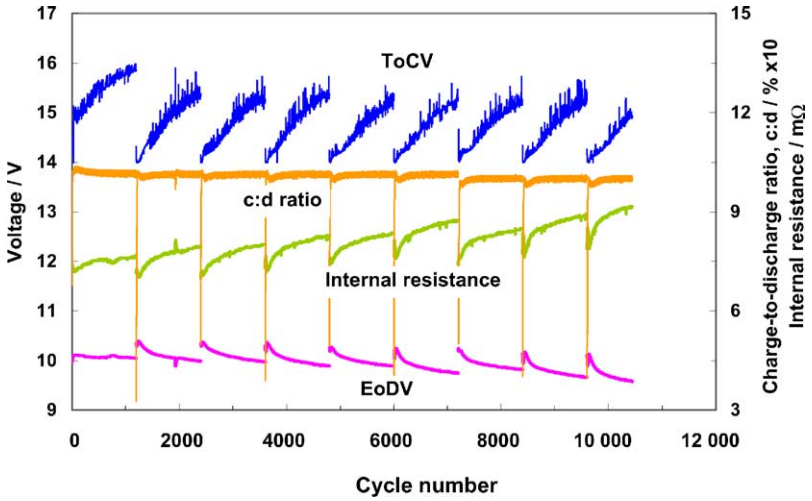

Fig. 4. Performance of VRLA battery VR2 under repetitive 42 V duty: ToCV, top-of-charge voltage; EoDV, end-of-discharge voltage.

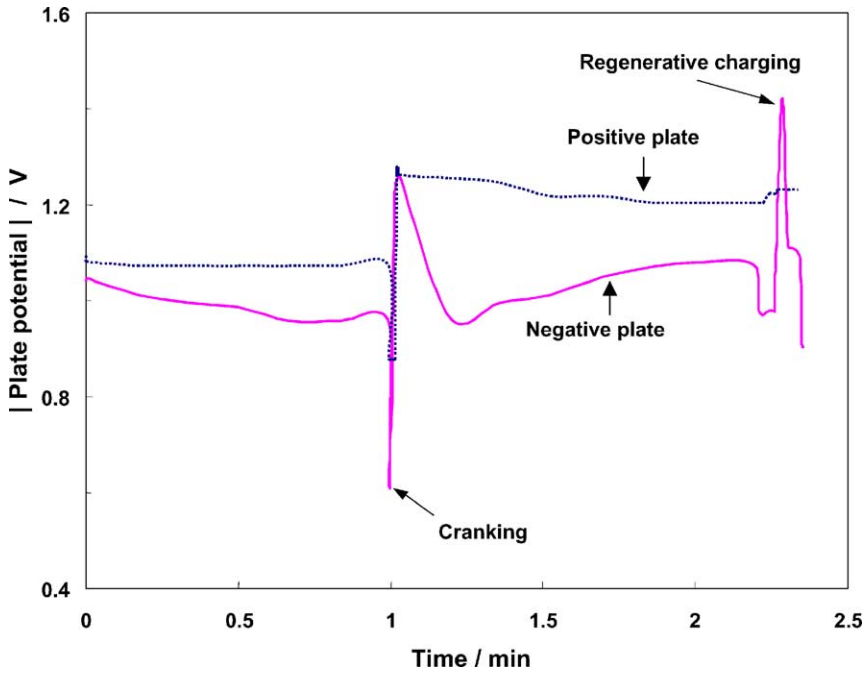

Fig. 5. Negative- and positive-plate potentials of VRLA battery VR2 during 6000th cycle of 42 V duty.

During discharge, the conversion of sponge lead to lead sulfate proceeds via two steps. First, the sponge lead at the negative plate reacts with HSO_4^- to form Pb^{2+}, SO_4^{2-} and H^+, i.e., the so-called 'dissolution process' (reaction (1)). Then, the Pb^{2+} combines with SO_4^{2-} to form $PbSO_4$, i.e., the so-called 'deposition process' or 'precipitation process' (reaction (2)). The first step is an electrochemical reaction and thus involves electron transfer. Such transfer of electrons takes place only on the conductive sites, i.e., on fresh lead. The rate of the electrochemical reaction is therefore dependent not only on the diffusion of HSO_4^- species, but also on the effective surface area of the sponge lead. On the other hand, the second step is a chemical reaction and proceeds at a rate which is acid-dependent. The solubility of lead sulfate does not increase with increase in sulfuric acid concentration [7]. Rather, it reaches a maximum value at a concentration of 10 wt.% sulfuric acid (1.07 relative density), and then decreases rapidly with further increase in concentration (Fig. 10). Thus, the Pb^{2+} will precipitate as lead sulfate at concentrations above the solubility curve. Clearly, for a given concentration of Pb^{2+} above $\sim 1\,mg\,l^{-1}$, the deposition (or precipitation) of Pb^{2+} to lead sulfate will be faster at plate locations which experience high concentrations of acid.

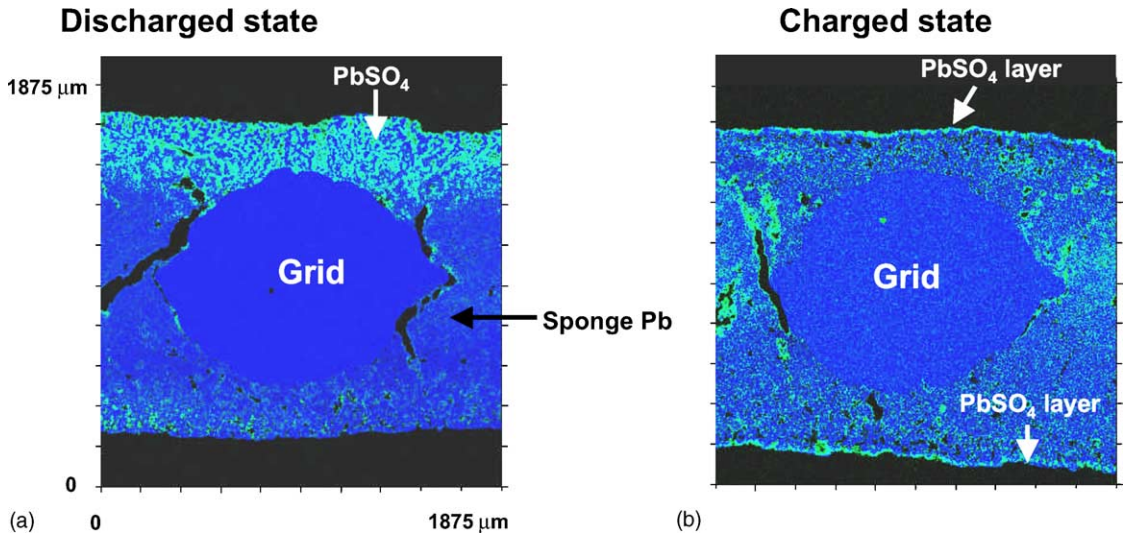

Fig. 6. Distribution of lead sulfate at central top of a negative plate taken from VRLA battery VR2 after failure.

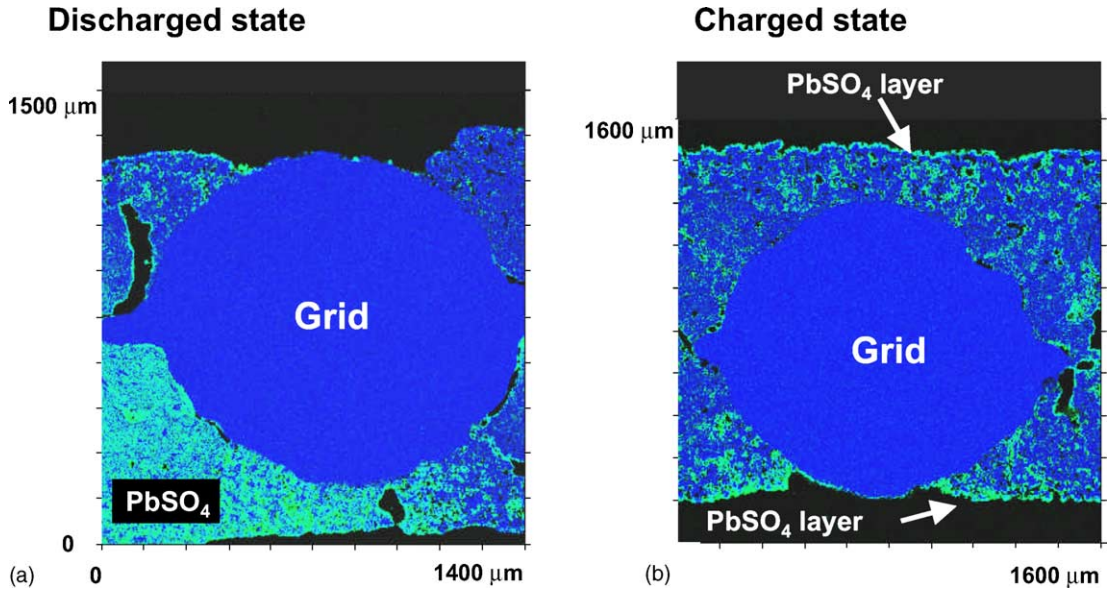

Fig. 7. Distribution of lead sulfate at central bottom of a negative plate taken from VRLA battery VR2 after failure.

During the initial stages of the discharge of a fully charged negative plate, electron transfer can take place at any location because the entire plate is conductive. Accordingly, the discharge process (both dissolution and deposition steps) occurs both on the surfaces and in the interior of the plate. Nevertheless, the reaction in the interior of the plate will soon slow down and/or stop, while that at the surfaces of the plate will continue. This is because less acid is now available in the interior.

The depth to which lead sulfate penetrates is dependent on the rate of discharge, as well as on the density and surface area of the plate. Paste density is the key factor in providing the macropores which are necessary for the transport of solution and ionic species to and from the reaction sites within the interior of the plate, while surface area provides sites for the current-generating electrochemical reaction. For the same paste density and surface area, the extent to which lead sulfate can penetrate is determined by the discharge rate.

Under low-rate discharge (i.e., $<0.4C_1$), the dissolution rate of Pb^{2+} from each lead crystal is slow and, therefore, the accompanying consumption of HSO_4^- in the interior of the plate is likely to be counterbalanced by the diffusion of HSO_4^- from the bulk of the electrolyte. Furthermore, the subsequent deposition of Pb^{2+} to $PbSO_4$ (reaction (2)) also occurs slowly due to the low supersaturation of Pb^{2+} in the vicinity of each parent lead crystal. (Note that, the deposition rate of $PbSO_4$ is proportional to the degree of supersaturation of Pb^{2+} in the sulfuric acid solution, i.e., the higher the supersaturation, the faster the deposition rate.) Since the rate of deposition (reaction (2)) is slow, newly formed $PbSO_4$

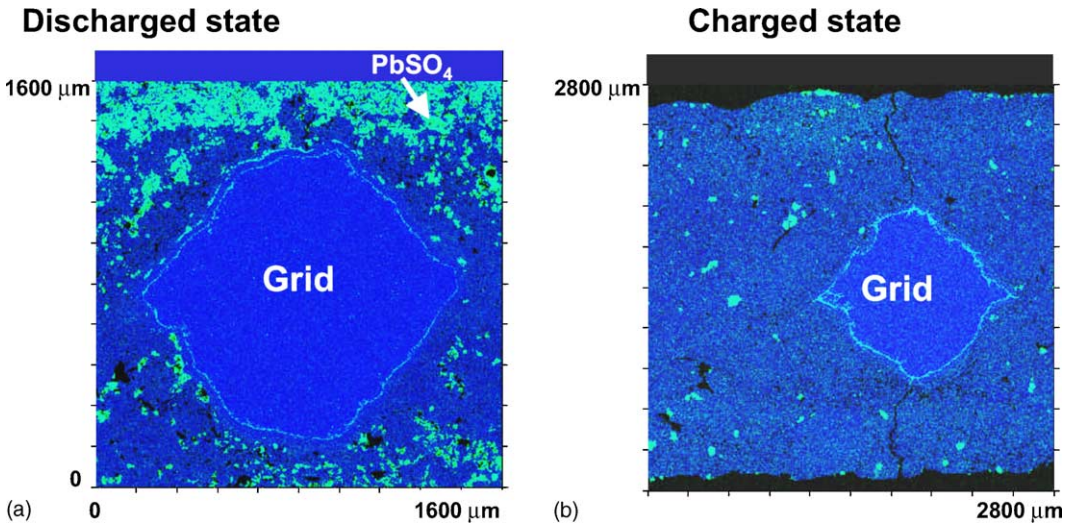

Fig. 8. Distribution of lead sulfate at central bottom of a positive plate taken from VRLA battery VR2 after failure.

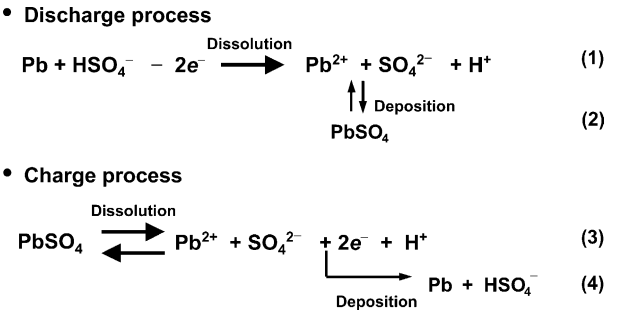

Fig. 9. Discharge and charge reactions at the negative plate of a lead-acid cell.

tends to precipitate preferentially on the already-deposited $PbSO_4$ crystals, i.e., growth rate > nucleation rate. Consequently, the deposited lead sulfate will continue to grow to various sizes of discontinuous crystals, both on the surface and in the interior of the negative plate. This form of lead sulfate is particularly desirable on the surface of the plate, as it provides an open structure that facilitates the ingress of HSO_4^- ions. Therefore, the discharge process can proceed deep into the interior of the plate. Accordingly, the lead sulfate develops evenly throughout the cross-section of the negative plate, as shown schematically in Fig. 11(a).

The formation of lead sulfate proceeds differently under high-rate discharge, e.g., under cranking-current ($\sim 18C_1$) conditions. The electrochemical reaction (i.e., reaction (1)) now proceeds so rapidly that the diffusion rate of HSO_4^- cannot catch up with the consumption rate. Consequently, lead sulfate forms mainly on the surface of the plate. Moreover, high-rate discharge generates a very high supersaturation of Pb^{2+} in the vicinity of each parent lead crystal. The lead sulfate will therefore precipitate quickly on any available surface, irrespective of whether this be sponge lead or already-deposited lead sulfate, i.e., nucleation rate > growth rate. Thus, a compact layer of tiny lead sulfate crystals will develop on the surface of the plate. This will reduce the effective surface area for electron transfer and will also hinder the diffusion of HSO_4^- into the interior of the plate (Fig. 11(b)). Under such conditions, the discharge reaction cannot proceed into the interior, but stops at the surface of the plate and at the walls of the pores.

During charging, the conversion of lead sulfate to sponge lead also proceeds via two reactions, namely, dissolution and deposition. Nevertheless, the nature of these reactions differs from that of the corresponding discharge reactions. Dissolution is now the chemical reaction, while the subsequent deposition is the electrochemical reaction. The lead sulfate first dissociates to Pb^{2+} and SO_4^{2+} ions (reaction (3)). The Pb^{2+} then receives to two electrons and reduces to lead (reaction (4)). Simultaneously, SO_4^{2+} combines with H^+ to form HSO_4^-. The electrons flow to the active sites in the negative-plate material via the grid members because the electrical resistance of the grid metal is much smaller than that of the discharged material. In addition to the reduction of Pb^{2+} to lead, there is the competing reaction of hydrogen evolution. Usually, hydrogen evolution only takes place near the end of charging for the following reasons: (i) most of the $PbSO_4$ has been converted to lead and, correspondingly, the sulfuric acid concentration, i.e., H^+ concentration, has increased; (ii) further dissolution of $PbSO_4$ to Pb^{2+} and SO_4^{2+} is slow. Having said this, hydrogen can also be involved during the early stages of the charging process, if the dissolution of $PbSO_4$ is hindered (v.i.).

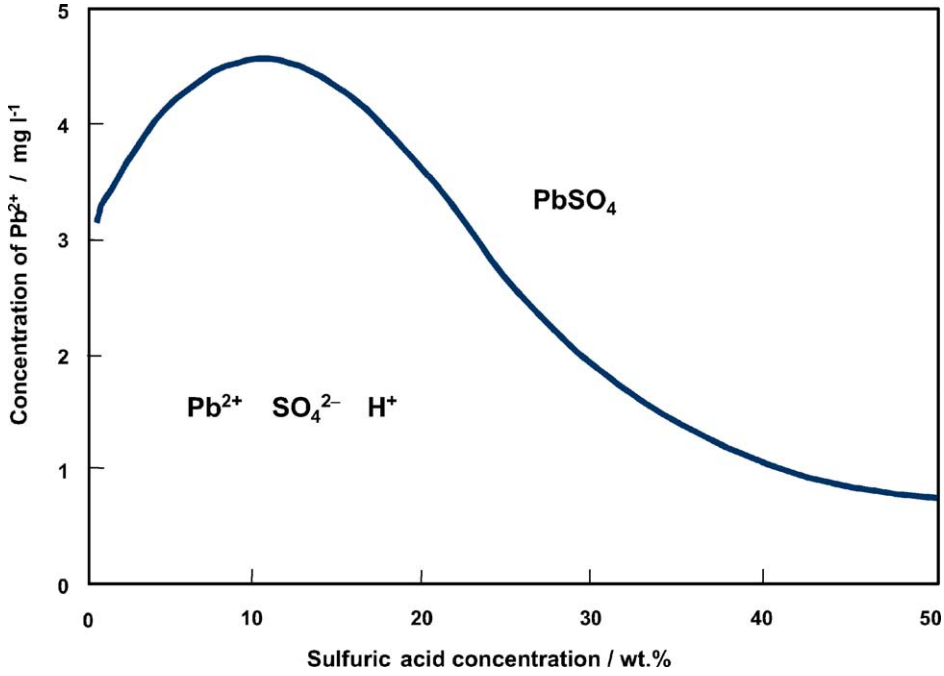

Fig. 10. Solubility curve for lead sulfate in sulfuric acid.

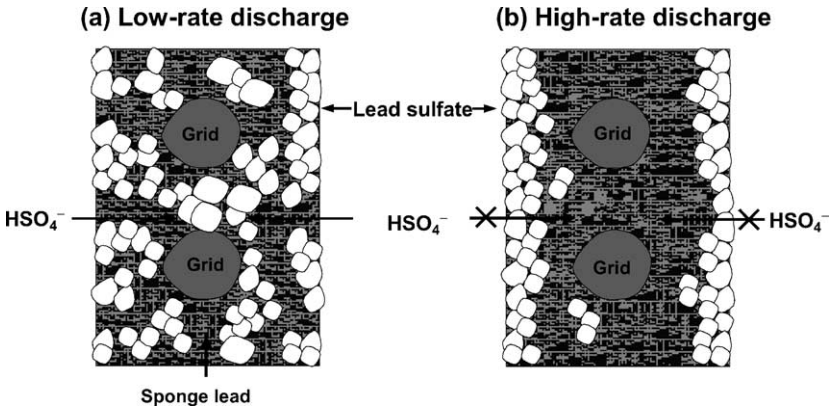

Fig. 11. Schematic representation of the distribution of lead sulfate in a negative plate subjected to: (a) low-rate or (b) high-rate discharge.

Having described the basic chemistry of the discharge–charge process, it is now appropriate to consider charging of the negative plate after it has been deeply discharged at a low rate. As discussed above, lead sulfate is formed throughout the entire cross-section of the plate and the relative density of the acid after discharge is low because of the high utilization of the active material. The dissolution of $PbSO_4$ to form Pb^{2+} and SO_4^{2-} increases at the low concentrations (see Fig. 10). Thus, the subsequent reduction of Pb^{2+} to sponge lead can take place smoothly before the evolution of hydrogen. With an overcharge of ~10%, the plate can be brought to a fully charged state without any difficulty. This is also true when the plate is subjected to low-rate PSoC cycling with equal amounts of charge input and charge output. In such duty, the state-of-charge of the negative plate decreases with cycling, but can be brought to 100% after the application of an equalization charge.

By contrast, charging of the negative plate after deep discharge at a high rate is difficult. Since high-rate discharge cannot proceed into the interior of the plate, but stops at the surface, the utilization of the active material is low. Consequently, the relative density of the acid after discharge is still at a high level and this decreases the dissolution of $PbSO_4$ (see Fig. 10). The lower concentration of Pb^{2+} will then impede the subsequent electrochemical reaction and, during the early stages of charging, will cause the negative-plate potential to become more negative to such extent that hydrogen can start to evolve. Furthermore, as mentioned above, the electrons flow from the grid members toward the surfaces of the plate. These electrons will reduce some hydrogen ions to hydrogen gas before reaching the lead sulfate layer, as shown schematically in Fig. 12. Thus, complete conversion of lead sulfate at the plate surface cannot be achieved, even with an overcharge of 10%, because of the combined effects of the early evolution of hydrogen and the oxygen-recombination reaction. In addition, the overcharge factor will increase with cycling because progressive water loss will dry-out the separator, increase the amount of oxygen reaching the plate, and hence will enhance the level of oxygen recombination. Thus, lead sulfate will accumulate on the surface of the negative plate and, eventually, the battery will be unable to provide sufficient power for engine cranking.

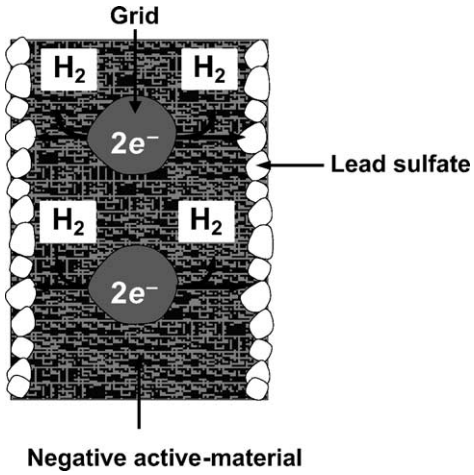

Fig. 12. Schematic representation of the charging process of a negative plate after high-rate discharge.

4. Conclusions

This study has identified the failure mode of VRLA batteries under HRPSoC cycling (42 V profile). The batteries fail due to the progressive accumulation of lead sulfate mainly on the surfaces of the negative plates. The sulfate layer develops to such an extent that the effective surface area of the plate is reduced markedly such that the plate can no longer deliver the high current required by the 42 V profile. High-rate discharge is the key factor which is responsible for the build-up of the lead sulfate layer. Discharging a battery at high rate causes a compact layer of tiny lead sulfate crystals to form on the surface of the negative plate. Subsequent charging gives rise to an early evolution of hydrogen and thus becomes less efficient. Hydrogen evolution is further exacerbated when a high charging current is used.

Acknowledgements

This work has been supported by the Advanced Lead-Acid Battery Consortium, Research Triangle Park, NC, USA.

References

[1] K. Peters, M.G. Mayer, D.A.J. Rand, in: Proceedings of the Fourth International Conference and Exhibition: Vehicle Electronic Systems 2001, Coventry, UK, June 27–28, 2001, ERA Report 2001-0214, Project 400059925, Paper 9.2, pp. 9.2.1–9.2.11.

[2] T. Noda, K. Hata, K. Yamanaka, K. Yamaguchi, M. Tsubota, Paper presented at the Proceedings of the Ninth Asian Battery Conference, Bali, Indonesia, September 2001.

[3] L.T. Lam, C.G. Phyland, D.A.J. Rand, A.J. Urban, ALABC Project C2.0, Novel Technique to Ensure Battery Reliability in 42 V PowerNets for New-generation Automobiles, Progress Report, August 2001–January 2002, CSIRO Energy Technology, Investigation Report ET/IR480R, March 2002, 19 pp.

[4] L.T. Lam, N.P. Haigh, C.G. Phyland, D.A.J. Rand, A.J. Urban, ALABC Project C 2.0, Novel Technique to Ensure Battery Reliability in 42 V PowerNets for New-generation Automobiles, Final Report, August 2001–November 2002, CSIRO Energy Technology, Investigation Report ET/IR561R, December 2002, 39 pp.

[5] L.T. Lam, N.P. Haigh, C.G. Phyland, T.D. Huynh, D.A.J. Rand, ALABC Project C 2.0, Novel Technique to Ensure Battery Reliability in 42 V PowerNets for New-generation Automobiles, Extended Report, January–April 2003, CSIRO Energy Technology, Investigation Report ET/IR604R, May 2003, 23 pp.

[6] R.H. Newnham, W.G.A. Baldsing, A.F. Hollenkamp, O.V. Lim, C.G. Phyland, D.A.J. Rand, J.M. Rosalie, D.G. Vella, ALABC Project C/N 1.1, Advancement of Valve-regulated Lead-acid Battery Technology for Hybrid-electric and Electric Vehicles, Final Report, July 2000–June 2002, CSIRO Energy Technology, Investigation Report ET/IR520R, August 2002, 44 pp.

[7] H. Bode, Lead-acid Batteries, Wiley, New York, USA, 1997, p. 27.